PROCEEDINGS OF THE ROYAL SOCIETY A MATHEMATICAL, PHYSICAL & ENGINEERING SCIENCES

On mobile assemblies of Bennett linkages

Y Chen and Z You

Proc. R. Soc. A 2008 **464**, 1275-1293
doi: 10.1098/rspa.2007.0188

PROCEEDINGS OF THE ROYAL SOCIETY A

Proc. R. Soc. A (2008) **464**, 1275–1293
doi:10.1098/rspa.2007.0188
Published online 19 February 2008

On mobile assemblies of Bennett linkages

By Y. Chen[1] and Z. You[2,*]

[1]*School of Mechanical and Aerospace Engineering, Nanyang Technological University, Singapore 639798, Republic of Singapore*
[2]*Department of Engineering Science, University of Oxford, Oxford OX1 3PJ, UK*

This paper deals with deployable structures formed by interconnected Bennett linkages. A total of eight cases that allow mobile assemblies of Bennett linkages being built have been found by considering the links that may contain sections with negative length. Among the eight assemblies, four are distinct ones, including the one that we reported previously, and the remaining can be obtained by modifying the four cases. All these assemblies consist of a grid of nested Bennett linkages. The layout of the assemblies can be repeated to form a large deployable structure. When the Bennett linkages are equilateral, the assemblies expand to form arches. For a non-equilateral case, the assemblies deploy into a helical shape with a cylindrical profile. They are geometrically overconstrained with a single degree of mobility. The newly found assemblies provide more choices in the design of deployable structures.

Keywords: Bennett linkage; overconstrained mechanism; mobile assembly; deployable structure

1. Introduction

The Bennett linkage (Bennett 1903, 1914) is a $4R$ spatial overconstrained linkage in which four rigid links are connected by four revolute joints (R) forming a closed loop. The axes of revolute joints are neither parallel nor concurrent to each other. In general, seven links are required to achieve a single degree of mobility for a loop assembly, according to the Kutzbach criterion (Beggs 1966). With only four links, the Bennett linkage is regarded as overconstrained and is the only known mobile linkage with a minimum number of links. Since its discovery, many publications have been dedicated to this remarkable linkage. One of the research focuses has been on the mathematical description and the kinematic characters of the linkage. For instance, Ho (1978) presented an approach to establish the geometric criteria for the existence of the Bennett linkage through the use of tensor analysis. Yu (1981) found that the links of the Bennett linkage were in fact two pairs of equal and opposite sides of a line symmetrical tetrahedron. Baker (1988) investigated the J-hyperboloid defined by the joint axes of the Bennett linkage and the L-hyperboloid defined by the links of the Bennett linkage. More recently, Huang (1997) showed that the screw axes of all possible coupler displacements of the linkage from any given configuration form a cylindroid. The other research focus is to construct $5R$ and $6R$ overconstrained

* Author for correspondence (zhong.you@eng.ox.ac.uk).

Received 23 August 2007
Accepted 23 January 2008

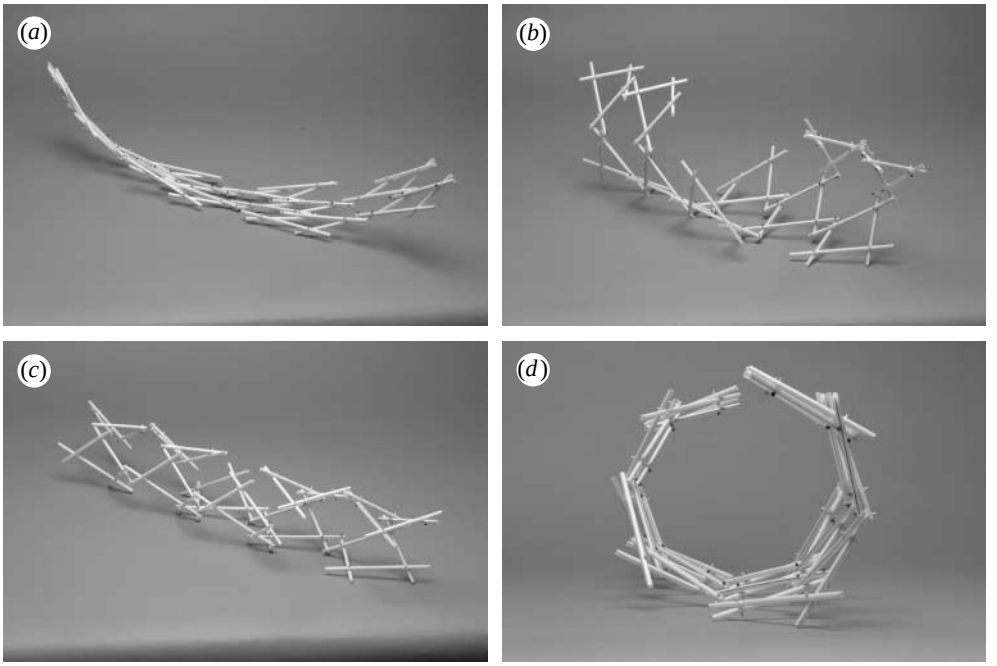

Figure 1. (*a–c*) Expansion sequence of an assembly based on the Bennett linkage and (*d*) the sectional view of the assembly.

linkages by merging several Bennett linkages. The most noticeable examples include the Myard linkage (Myard 1931), the Goldberg $5R$ and $6R$ linkages (Goldberg 1943), the Waldron hybrid linkage (Waldron 1968), the Bennett-joint $6R$ linkage (Mavroidis & Roth 1994), the Dietmaier $6R$ linkage (Dietmaier 1995) and Wohlhart's double-Goldberg linkages (Wohlhart 1991). These linkages still retain the single degree of freedom as the original Bennett linkage. A summary was provided by Chen (2003).

A few years ago, we reported the discovery of a family of mobile assemblies based on the Bennett linkage (Chen & You 2005). The findings allow us to construct not only a large mobile grid with an arch or spiral profile, but also towers, as well as more complex mobile assemblies, all of which are over-constrained with a single degree of mobility. One such structure is shown in figure 1.

This paper is a continuation of our previous work. We have discovered that it is possible to obtain new assemblies of Bennett linkages by considering that sections of a link may have a negative length. All of our findings have been verified by physical models. The new assemblies provide a much large scope in the design of deployable structures for civil and aerospace applications.

The layout of the paper is as follows. Section 2 gives a brief introduction of Bennett linkage and its basic assembly. In §3, we define the negative link length and, by adopting such lengths, several new assemblies can be derived from the basic ones. The comparisons among the various assemblies are discussed in §4. Finally, the conclusions and further discussion are given in §5.

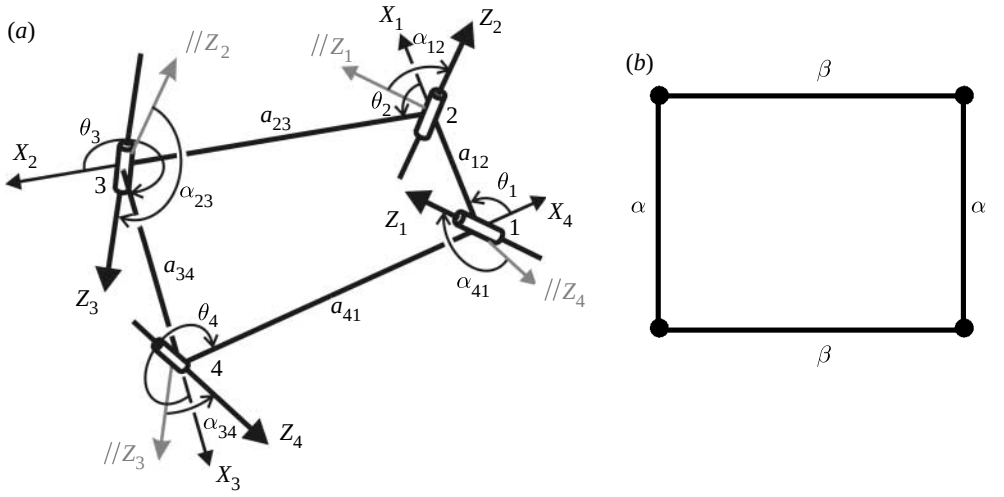

Figure 2. (*a*) A Bennett linkage and (*b*) its schematic.

2. Bennett linkages and the basic assembly

We call the mobile assemblies that were discovered previously the *basic assemblies*. To understand how they are constructed, it is necessary to review briefly the conditions for a $4R$ Bennett linkage to have a single degree of mobility. Let us build a Bennett linkage in which each of the links is normal to the axes of the two revolute joints it bridges. Thus, the *length* of a link is therefore defined as the distance between the axes and the *twist* as the skewed angle between the axes. The linkage is shown in figure 2*a*, whose link lengths are therefore a_{12}, a_{23}, a_{34} and a_{41} as well as twists α_{12}, α_{23}, α_{34} and α_{41}. To define the positive sense for these parameters, a coordinate system at each joint needs to be set up. To do so, we first let Z_i be the axes of revolute joint j ($j=1$, 2, 3 and 4). X_j is the axis normal to both Z_j and Z_{j+1}, positively from joints j to $j+1$ (when $j+1$ becomes 5, it is replaced by 1). $a_{j\,j+1}$ is the distance between axes Z_j and Z_{j+1}, which is also referred to as the length of link from joints j to $j+1$. $\alpha_{j\,j+1}$ is the twist of the same link, which is the angle from axes Z_j to Z_{j+1} positively about X_j. In figure 2*a*, axis $//Z_j$, which is parallel to Z_j, is drawn at joint $j+1$ in grey so that the twist can be shown clearly. The motion of the linkage is determined by kinematic variables θ_j, which is the angle of rotation from X_{j-1} to X_j positively about Z_j (when subscript $j-1=0$, it is replaced by 4).

The mobility conditions are as follows (Beggs 1966).

(a) Two alternate links have the same length and the same twist, i.e.

$$a_{12} = a_{34} = a, \qquad a_{23} = a_{41} = b, \tag{2.1a}$$

$$\alpha_{12} = \alpha_{34} = \alpha, \qquad \alpha_{23} = \alpha_{41} = \beta. \tag{2.1b}$$

(b) Lengths and twists should satisfy the condition

$$\frac{\sin\alpha}{a} = \frac{\sin\beta}{b}. \tag{2.1c}$$

The closure equations of linkage are

$$\theta_1 + \theta_3 = 2\pi, \qquad \theta_2 + \theta_4 = 2\pi \tag{2.2a}$$

and

$$\tan\frac{\theta_1}{2}\tan\frac{\theta_2}{2} = \frac{\sin\frac{1}{2}(\alpha_{23}+\alpha_{12})}{\sin\frac{1}{2}(\alpha_{23}-\alpha_{12})}, \tag{2.2b}$$

which ensure that only one of the θ's is independent, so the linkage has a single degree of mobility (Baker 1979).

Taking $\theta_1 = \theta$ and $\theta_2 = \varphi$, equation (2.2*b*) becomes

$$\tan\frac{\theta}{2}\tan\frac{\varphi}{2} = \frac{\sin\frac{1}{2}(\beta+\alpha)}{\sin\frac{1}{2}(\beta-\alpha)}. \tag{2.3}$$

For easy description, we adopt the schematic in figure 2*b* to represent a Bennett linkage, though it is necessary to bear in mind that it is in fact a three-dimensional linkage. In that figure, the four links are illustrated by solid lines, and four revolute joints are located at the intersections of the lines, represented by circular solid dots. The twists of the joint axes along a link are denoted by α and β, respectively, which are marked alongside the link connecting the joints. The lengths of links are not given in the diagram, but it will not affect the generality, as long as we bear in mind that the opposite sides always have equal lengths, the link lengths corresponding to twists α and β are a and b, respectively, and $a/b = \sin\alpha/\sin\beta$ due to (2.1*c*).

A typical mobile assembly of the Bennett linkages reported by Chen & You (2005) is shown in figure 3*a*, where each of the rectangles represents a Bennett linkage and each of the straight lines represents a single rigid link that contains four revolute joints, two at each end and two in the middle of the link. In order to make the assembly mobile, it must be satisfied that, along the diagonal lines from top left to bottom right, all of the Bennett linkages have the same twists α_i and β_i (or $-\alpha_i$ and $-\beta_i$). To be precise, these diagonal lines, shown as the grey dashed-dot lines in figure 3*a*, are the lines formed by linking relevant joints diagonally. Let us name them the *guidelines* and use i ($i=1,2,\ldots$) for each individual guideline. For the Bennett linkages on the different guidelines, the following condition must be met:

$$\frac{\sin\alpha_i}{\sin\beta_i} = k, \tag{2.4}$$

where k is a constant throughout the whole assembly. Owing to equations (2.1*c*) and (2.4), the ratio between two lengths of links must be the same for all the Bennett linkages in the assembly. In other words, all of the rectangles are similar to that shown in figure 2*b*.

In general, the assembly deploys into a cylindrical profile. During deployment, the guidelines remain straight and parallel. They expand along the longitudinal direction of the cylinder. Along the other diagonal directions, that is, the direction from top right to bottom left, the structure generally distorts spirally on the surface of the cylinder.

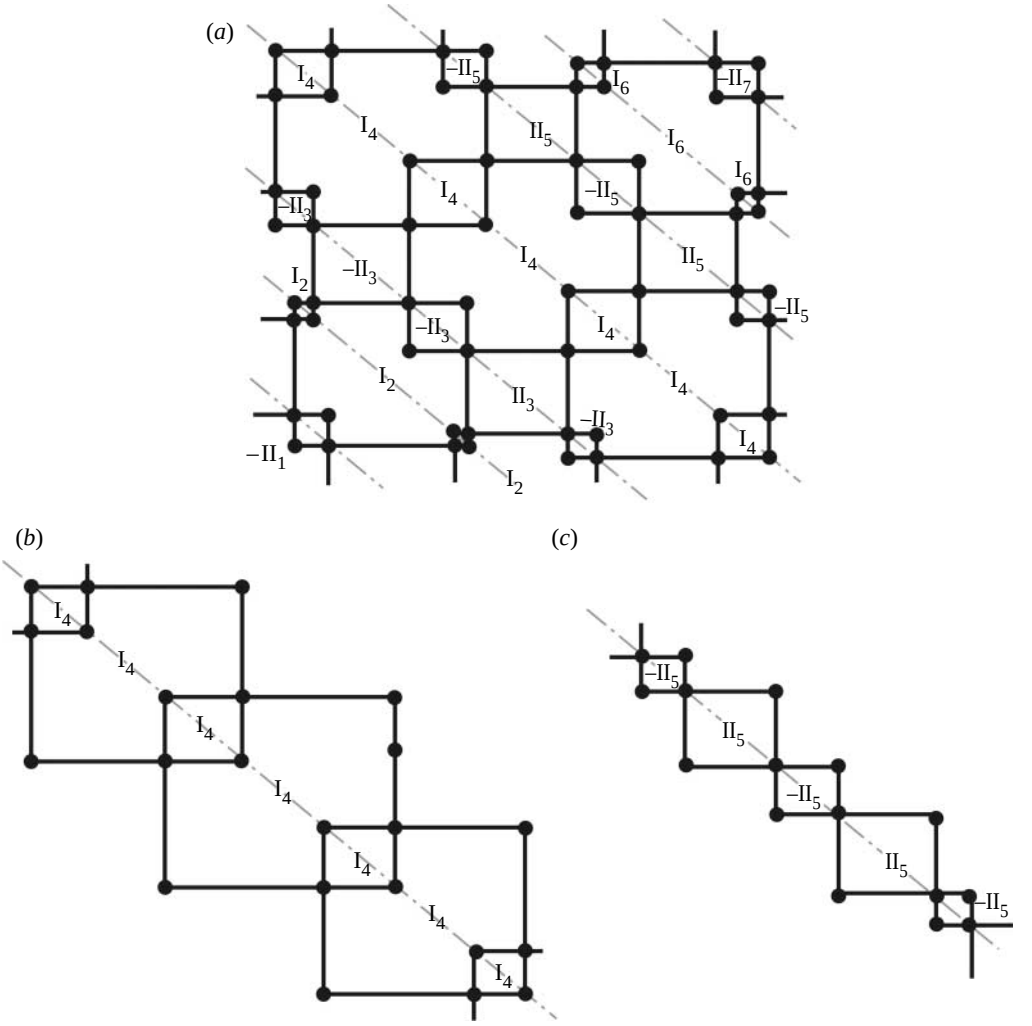

Figure 3. Schematic of assembly of similar Bennett linkages and its guidelines. (*a*) Whole assembly, (*b*) linkages on type I guideline and (*c*) linkages on type II guideline.

The guidelines can be further classified into type I and II lines. Along a type I line, all of the larger Bennett linkages, marked as I_i in figure 3*b*, are interconnected by the smaller Bennett linkages. The twists must be the same for both the large and small Bennett linkages, which are denoted by α_i and β_i. Along a type II line, all of the Bennett linkages, marked as II_i or $-\mathrm{II}_i$ in figure 3*c*, are connected through their corners, sharing the two common links. The twists for the Bennett linkages are α_i and β_i or $-\alpha_i$ and $-\beta_i$, alternating between the adjacent Bennett linkages. For the Bennett linkages whose twists are $-\alpha_i$ and $-\beta_i$, we denote them by $-\mathrm{II}_i$.

3. The possible mobile assemblies

A typical link in the basic assembly, i.e. the assembly introduced in §2, has four revolute hinges. Denote the locations of the end joints by A, B, C and D, and

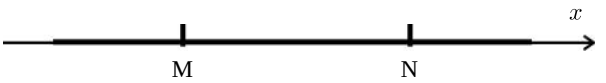

Figure 4. Definition of the positive length.

Table 1. Eight possible cases for a three section link.[a]

case		AB	BC	CD	AD	diagram of a link[a]
1	length sign	+	+	+	+	μ ν $-\nu$ A B C D
	physical twist	μ	ν	$-\nu$	μ	
2	length sign	−	+	+	+	$-\mu$ $\mu+\nu$ $-\nu$ B A C D
	physical twist	$-\mu$	ν	$-\nu$	μ	
3	length sign	+	+	−	+	μ 0 ν A B D C
	physical twist	μ	ν	ν	μ	
4	length sign	+	−	+	+	$\mu+\nu$ $-\nu$ 0 A C B D
	physical twist	μ	$-\nu$	$-\nu$	μ	
5	length sign	−	+	−	+	$-\mu$ μ ν B A D C
	physical twist	$-\mu$	ν	ν	μ	
6	length sign	+	−	−	+	μ ν $-\nu$ A D C B
	physical twist	μ	$-\nu$	ν	μ	
7	length sign	−	−	+	+	$-\nu$ $-\mu$ μ C B A D
	physical twist	$-\mu$	$-\nu$	$-\nu$	μ	
8	length sign	−	−	−	−	ν $-\nu$ $-\mu$ D C B A
	physical twist	$-\mu$	$-\nu$	ν	$-\mu$	

[a]The twist marked on the link is the physical twist between two adjacent joints from left to right along the link.

the shortest distances among the joints by AB, BC, CD and DA. These distances are called the section lengths of a link. In the basic assembly, all of the lengths are positive. However, this can be altered.

Before we embark upon deriving the formulae for new mobile assemblies, let us define the positive and negative length. First, assume the x-axis is collinear with a link (figure 4). Take two points, M and N on the x-axis with a positive direction. If $x_N - x_M > 0$, then length MN is positive. Meanwhile, the corresponding twist μ_{MN} is the skew angle between the axes of the revolute joints at M to N positively about the x-axis. If MN is negative, the corresponding twist becomes μ_{NM} or $-\mu_{MN}$.

For any of the links in the basic assembly, commonly for twists there must be

$$\alpha_{AB} = \alpha_{AD} = \mu \quad \text{and} \quad \alpha_{BC} = -\alpha_{CD} = \nu,$$

when AB, BC and CD are all positive, and μ and ν can be α's or β's, depending on the locations of the link.

It has been discovered that the lengths can be positive as well as negative. There are totally eight ($=2^3$) possible combinations of the sections with positive and negative lengths, termed as cases 1–8, all of which are listed in table 1. In order to retain mobility, the twists need to be adjusted accordingly if some of the lengths become negative.

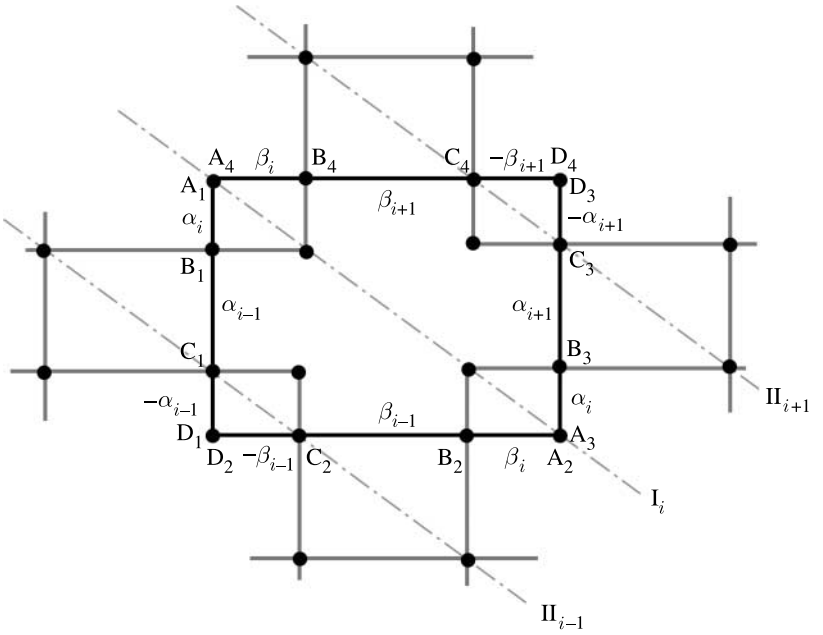

Figure 5. A typical Bennett linkage in a case 1 assembly.

Case 1. Case 1 is, in fact, the basic assembly. Consider a typical Bennett linkage in the assembly. It has four links, A_1D_1, A_2D_2, A_3D_3 and A_4D_4 that are connected in such a way that D_1 is connected with D_2, A_2 with A_3, etc. (figure 5). To form an assembly, the top left corner of the Bennett linkage is connected to its neighbouring Bennett linkage at B_1 and B_4, forming a smaller I_i linkage, as does the bottom right corner. At the top right and bottom left corners, it is also connected with adjacent Bennett linkages, forming two smaller Bennett linkages II_{i-1} and II_{i+1} with twists of either $-\alpha_{i-1}$ and $-\beta_{i-1}$ or $-\alpha_{i+1}$ and $-\beta_{i+1}$, respectively. A model is shown in figure 6 which demonstrates that the assembly has a single degree of mobility.

Case 2. In case 2, only section AB of a link has a negative length (table 1). A typical Bennett linkage is shown in figure 7*a*, which is formed by connecting four links at A's and D's. The twists of each link are as follows:

$$\left.\begin{aligned} \alpha_{A_1D_1} &= -\alpha_{B_1A_1} = \alpha_{A_3D_3} = -\alpha_{B_3A_3} = \alpha_i, \\ \alpha_{A_2D_2} &= -\alpha_{B_2A_2} = \alpha_{A_4D_4} = -\alpha_{B_4A_4} = \beta_i, \end{aligned}\right\} \tag{3.1a}$$

$$\alpha_{B_1C_1} = -\alpha_{C_1D_1} = \alpha_{i-1} \quad \text{and} \quad \alpha_{B_2C_2} = -\alpha_{C_2D_2} = \beta_{i-1}, \tag{3.1b}$$

$$\alpha_{B_3C_3} = -\alpha_{C_3D_3} = \alpha_{i+1} \quad \text{and} \quad \alpha_{B_4C_4} = -\alpha_{C_4D_4} = \beta_{i+1}. \tag{3.1c}$$

Similar to the previous case, a number of small Bennett linkages are formed through joints at B's and C's, and a complete assembly is shown in figure 7*b*. Owing to the particular twists given in (3.1*a*)–(3.1*c*), in this assembly, all of the guidelines are type II. The large Bennett linkages do not overlap along these

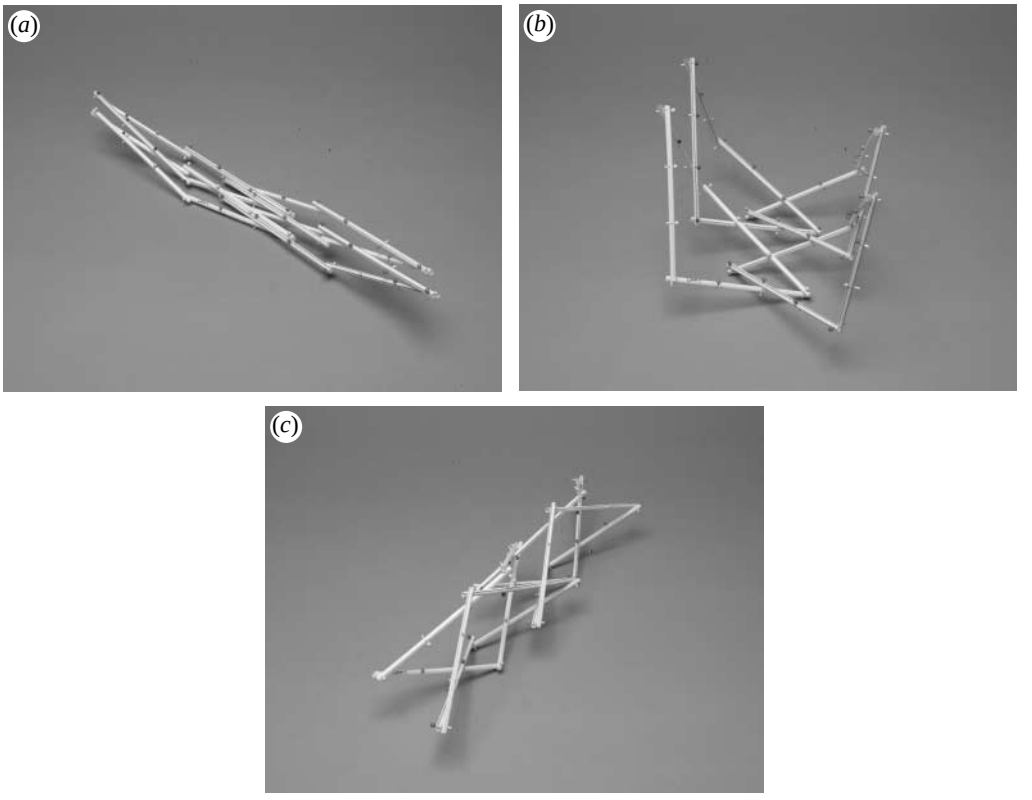

Figure 6. (*a–c*) Deployment sequence of a case 1 model.

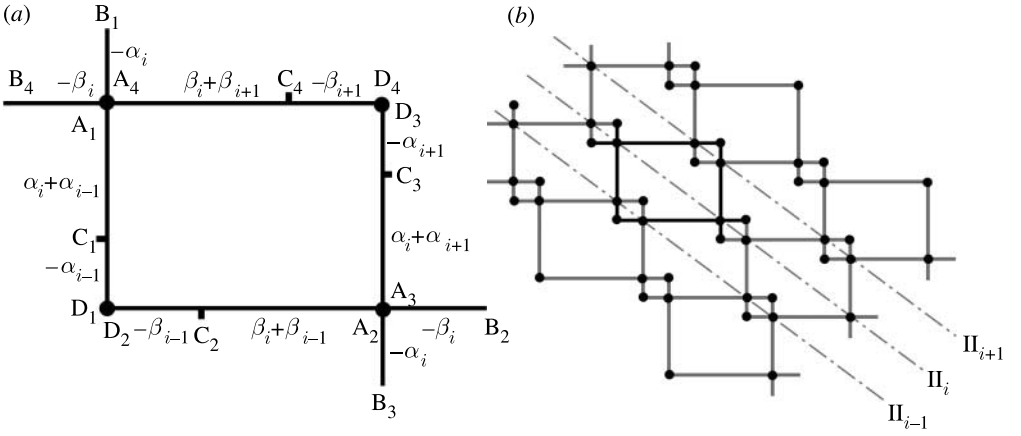

Figure 7. Construction of a case 2 assembly. (*a*) A typical linkage and (*b*) its assembly.

guidelines, but they do along the diagonals from top right to bottom left. When all of the twists satisfy the mobile condition (2.4), this assembly is mobile, which is verified by the model shown in figure 8.

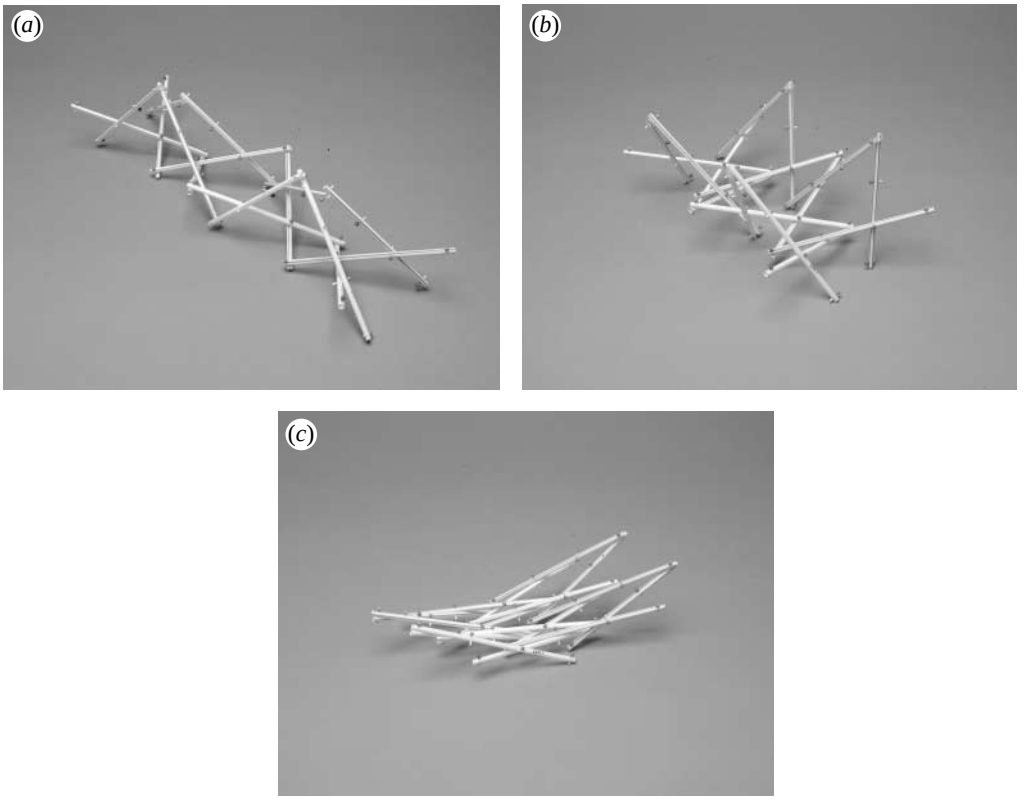

Figure 8. (*a–c*) Deployable sequence of a case 2 model.

Case 3. In this case, only section CD has a negative length (table 1). For the Bennett linkage, formed by connecting four links at A's and D's, the twists of each link are as follows:

$$\left.\begin{aligned}\alpha_{A_1D_1} = \alpha_{A_1B_1} = \alpha_{A_3D_3} = \alpha_{A_3B_3} = \alpha_i,\\ \alpha_{A_2D_2} = \alpha_{A_2B_2} = \alpha_{A_4D_4} = \alpha_{A_4B_4} = \beta_i,\end{aligned}\right\} \tag{3.2a}$$

$$\alpha_{B_1C_1} = \alpha_{D_1C_1} = \alpha_{i-1} \quad \text{and} \quad \alpha_{B_2C_2} = \alpha_{D_2C_2} = \beta_{i-1}, \tag{3.2b}$$

$$\alpha_{B_3C_3} = \alpha_{D_3C_3} = \alpha_{i+1} \quad \text{and} \quad \alpha_{B_4C_4} = \alpha_{D_4C_4} = \beta_{i+1}. \tag{3.2c}$$

These twists are shown in figure 9*a*.

The entire assembly can be obtained by connecting a number of Bennett linkages together at B's and C's. A schematic of the assembly is given in figure 9*b*. It is interesting to note that all of the guidelines are now type I due to the fact that all of the twists have the same signs (table 1). The Bennett linkages overlap along the guidelines I_{i-1}, I_i, I_{i+1}, etc., but they do not overlap at all along the diagonals from top right to bottom left. Again, when all the twists satisfy the mobile condition (2.4), this assembly becomes mobile, which is demonstrated by the model shown in figure 10.

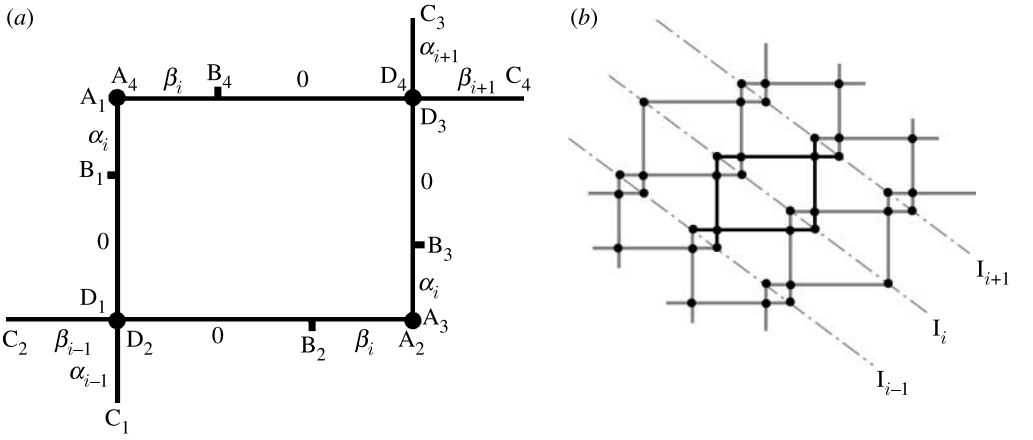

Figure 9. Construction of a case 3 assembly. (*a*) A typical linkage and (*b*) its assembly.

Case 4. The length of section BC is negative in this case. The corresponding twists, listed in table 1, are given in figure 11*a* for the Bennett linkage obtained by connecting at A's and D's. They are

$$\left.\begin{aligned}\alpha_{A_1D_1} = \alpha_{A_1B_1} = \alpha_{A_3D_3} = \alpha_{A_3B_3} = \alpha_i,\\ \alpha_{A_2D_2} = \alpha_{A_2B_2} = \alpha_{A_4D_4} = \alpha_{A_4B_4} = \beta_i,\end{aligned}\right\} \tag{3.3a}$$

$$\alpha_{C_1B_1} = \alpha_{C_1D_1} = -\alpha_{i-1} \quad \text{and} \quad \alpha_{C_2B_2} = \alpha_{C_2D_2} = -\beta_{i-1}, \tag{3.3b}$$

$$\alpha_{C_3B_3} = \alpha_{C_3D_3} = -\alpha_{i+1} \quad \text{and} \quad \alpha_{C_4B_4} = \alpha_{C_4B_4} = -\beta_{i+1}. \tag{3.3c}$$

A number of such linkages can be connected at B's and C's to form a large assembly; however, the situation is a little more complex than the cases discussed earlier. Let us show how this is carried out by considering connections along the guidelines. Firstly, when a few linkages are connected at B's, all of them stay on the same type I diagonal, as shown in figure 11*b*. Note that at a few places the links cross over each other but they are not joined. These places therefore do not have circular solid dots that have been used to indicate a hinged connection. Owing to (3.3*a*), the Bennett linkages overlap, forming some intermediate ones in between. All of the linkages have the same twists α_i and β_i along diagonal I_i. Secondly, when several linkages are connected at C's, the assembly forms a curved profile in the diagonal direction from top right to bottom left (figure 11*c*). Again, some of the links cross over in the schematics, but they are, in fact, not joined. Owing to (3.3*b*) and (3.3*c*), the linkages EFGH and PQST have twists of $-\alpha_{i-1}$, $-\beta_{i-1}$ and $-\alpha_{i+1}$, $-\beta_{i+1}$, respectively. So when the linkages are joined at both B's and C's, we obtain the assembly shown in figure 11*d*. Note that, although all of the guidelines are type I in the assembly, along I_{i-1}, the linkages EFGH and IJKL, as well as IMGN, have twists of $-\alpha_{i-1}$ and $-\beta_{i-1}$ owing to (3.3*b*), and along I_{i+1}, the linkages PQST and RUVW, as well as RXSY, have twists of $-\alpha_{i+1}$ and $-\beta_{i+1}$ owing to (3.3*c*). For all of the twists here that have a negative sign, the corresponding guidelines are type I instead of type II. When all

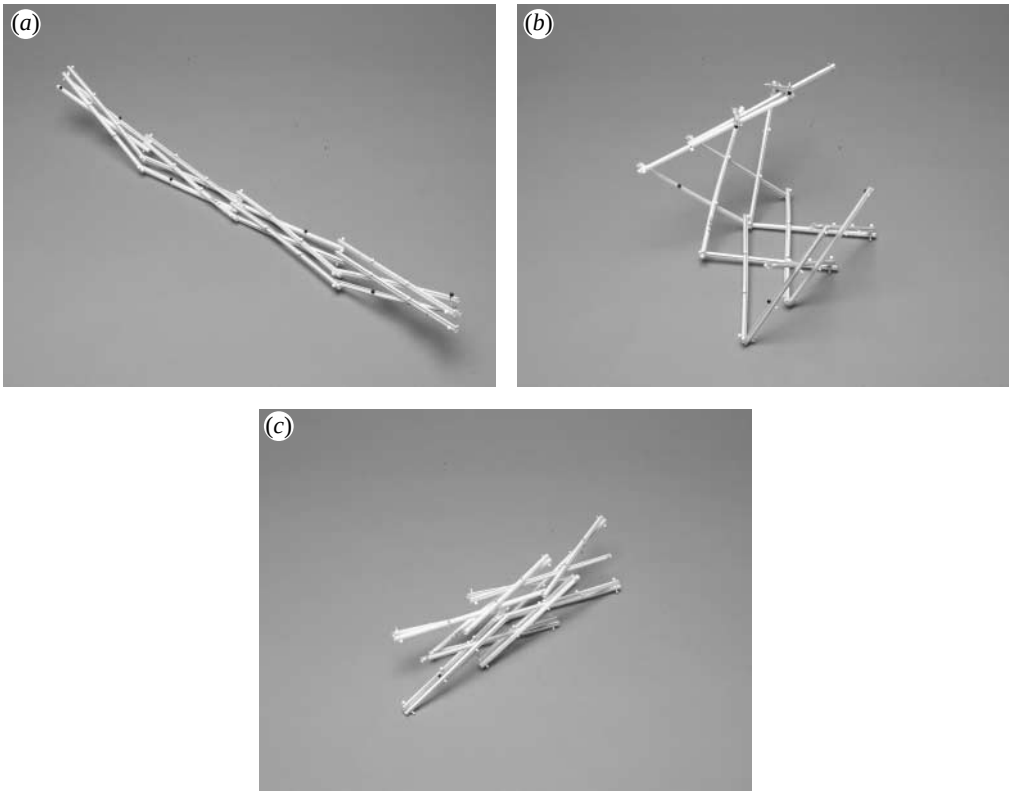

Figure 10. (*a–c*) Deployable sequence of a case 3 model.

the twists meet the mobile condition (2.4), this assembly becomes mobile (see the model in figure 12). However, owing to the large overlap, there could be conflicts during the deployment. For example, the corners Q and H in the centre of the assembly in figure 11*c* may be in collision with each other. But the same is not true for the similar corners in figure 11*b*, because the overlap of two Bennett linkages are connected along a type I_i guideline in which one of the corners moves up, whereas the other goes down during deployment. This feature has been used by Chen & You (2005) to construct multilayer assemblies.

Cases 5–8. The assemblies of cases 5–7 are shown in figures 13–15, in which the typical Bennett linkage is drawn in black. They all have type I and II guidelines altered from one to another. The largest Bennett linkages in the assemblies in cases 5–7 are the same as the typical Bennett linkage in case 1. But, the places where the linkages are connected with the neighbouring ones are different because the negative section lengths have switched A, B, C or D. If we regard the largest rectangles in the assemblies as the typical Bennett linkage instead, the three assemblies based on cases 5–7 are similar to that in case 1.

For case 8, the lengths of all of the sections are negative, which are symmetric to case 1 where the direction of the guidelines is altered from top right to bottom left (figure 16).

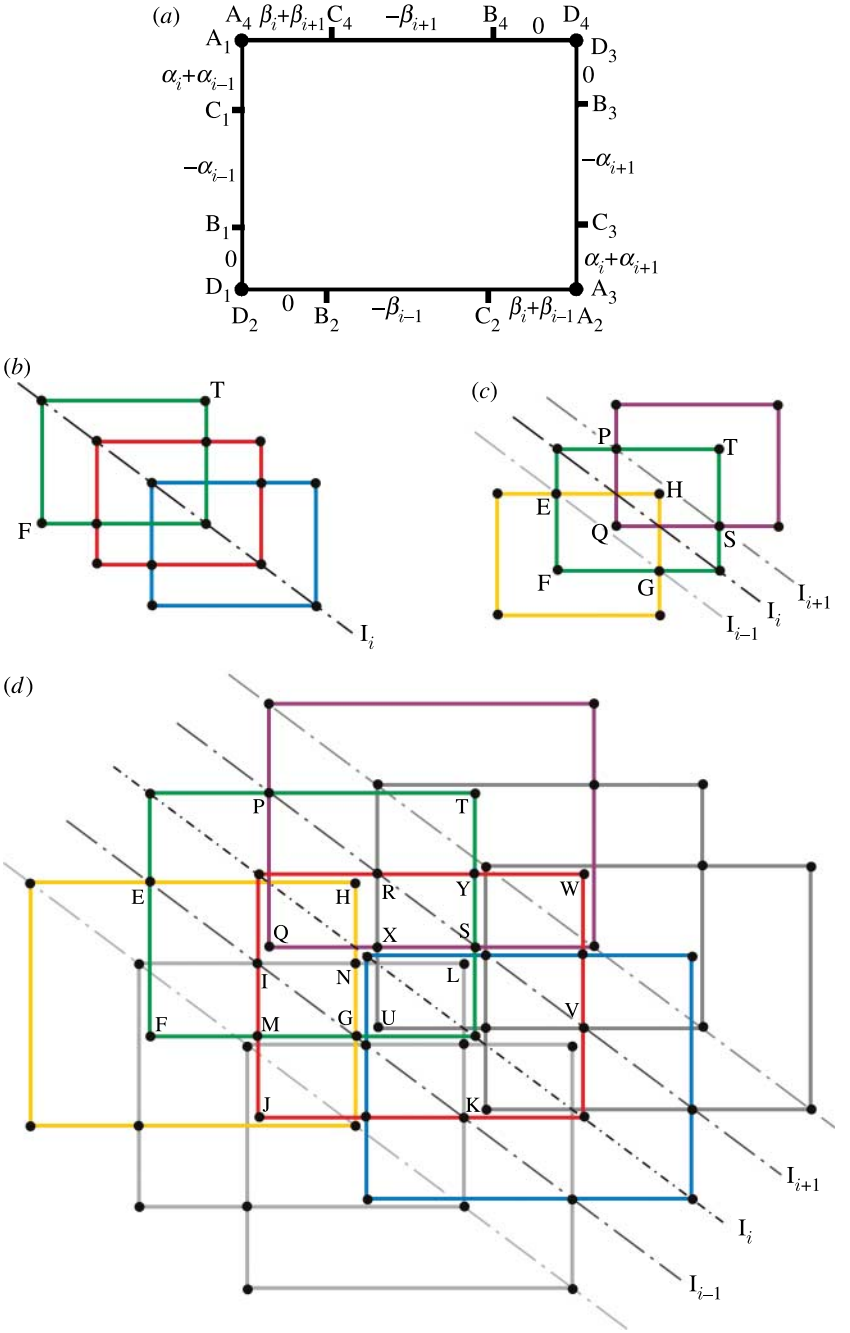

Figure 11. Construction of a case 4 assembly. (*a*) A basic unit. (*b*) Connection of linkages along the guideline and (*c*) in the other diagonal direction. (*d*) The whole assembly.

All of these four assemblies will be mobile when the twists meet the mobile condition (2.4).

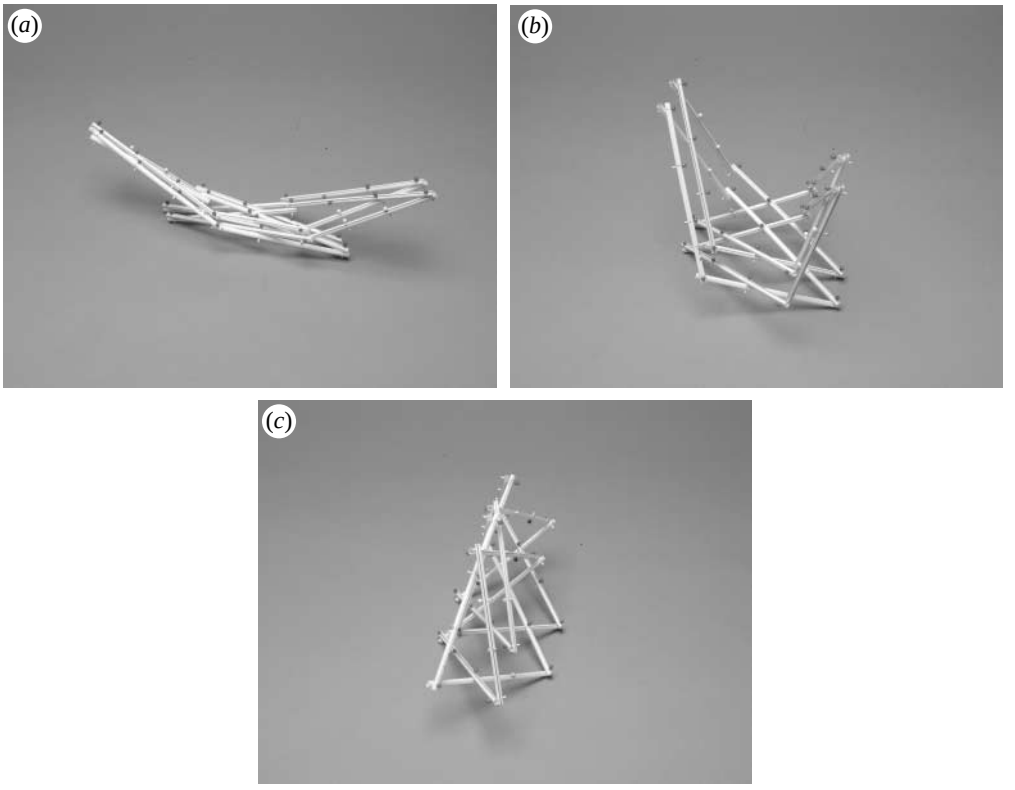

Figure 12. (*a–c*) Deployable sequence of a case 4 model.

4. Comparison of different assemblies

Although a total of eight cases have been presented in §3, not all of them are independent. Considering the twists along a single link, it can be found that the order of twists along a single link for cases 5–8 is the same as the one for case 1 after suitable variable substitution (table 1). Moreover, the largest Bennett linkages in the assemblies based on cases 5–8, represented by the largest rectangles in figures 13–16, are also similar to those in case 1. Hence, only cases 1–4 are independent.

In general, all of the assemblies of cases 1–8 deploy spirally to form a cylindrical profile. The helical shape is determined by the dimension of the typical Bennett linkage whose property is determined by (2.1*a*)–(2.1*c*). If $a > b$, the assembly deploys to a left-handed helical, whereas if $a < b$, it deploys to a right-handed one. When $a = b$, it forms an arch. The guidelines remain straight and parallel all the time. In this section, the geometry of four distinct assemblies of cases 1–4 will be compared.

In order to make a meaningful comparison of four assemblies, the following geometric preconditions are set up to make the total length of links in the assemblies equal to each other.

(i) Each assembly consists of nine typical Bennett linkages arranged three in a row with three rows in total (figure 17*a*). Smaller intermediate Bennett linkages are not accounted for here.

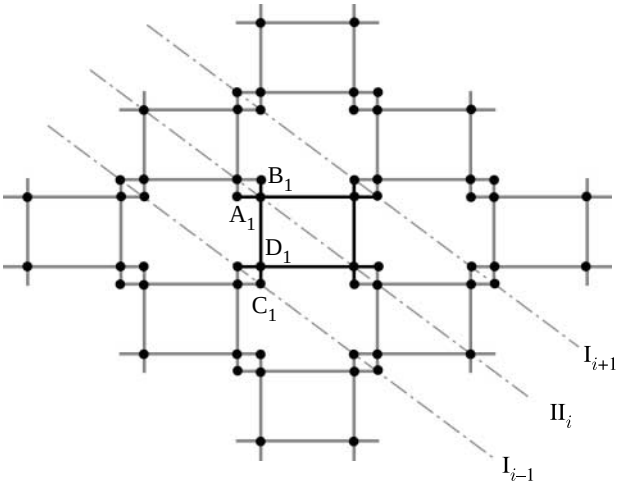

Figure 13. A case 5 assembly.

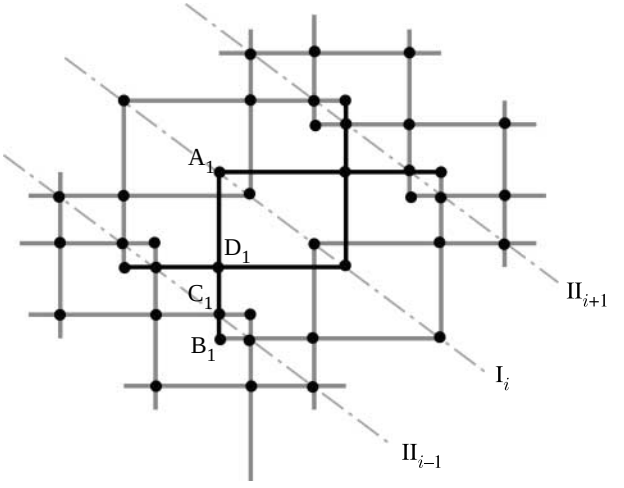

Figure 14. A case 6 assembly.

(ii) The lengths of the links in the typical Bennett linkages are a and b. Each link is divided into three equal sections, with section lengths being $a/3$ and $b/3$, respectively.

(iii) The twists of each Bennett linkage are either α and β or $-\alpha$ and $-\beta$. The lengths and twists satisfy the geometric condition of the Bennett linkage (2.1c) and mobility condition for the assemblies (2.4).

Based on the above preconditions, the distance between two rows along the guideline, l, and the radius of the cylindrical profile, r, can be calculated. Both l and r are indicated in figure 17a,b, respectively.

To obtain l and r, we need to study the geometry of a typical Bennett linkage in three-dimensional space first. Figure 18a shows a Bennett linkage ABCD being placed on a cylindrical surface in such a way that A, B, C and D are on the surface

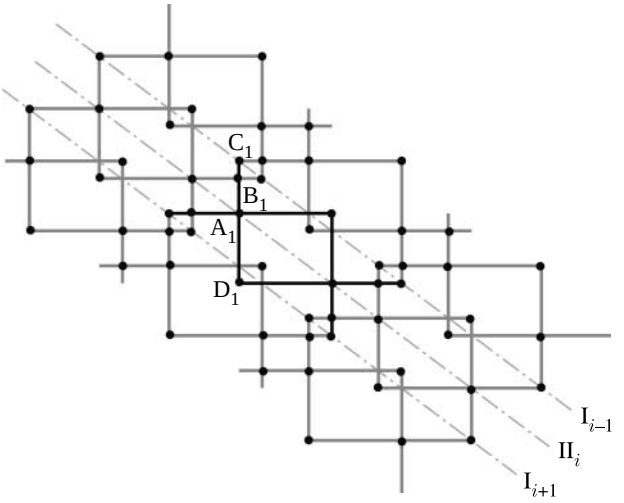

Figure 15. A case 7 assembly.

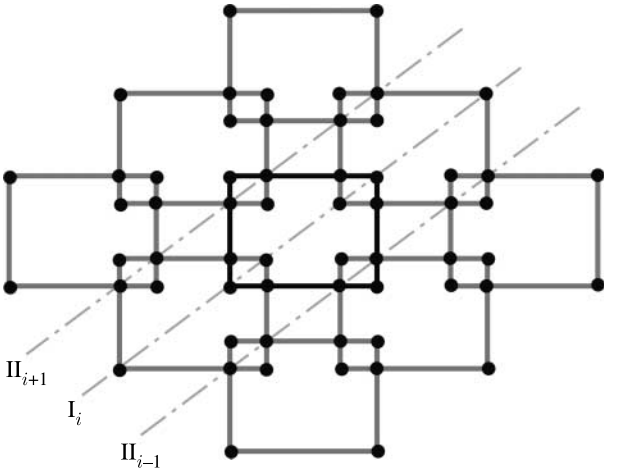

Figure 16. A case 8 assembly.

and line BD, which is collinear with a guideline, is along the longitudinal direction of the cylinder. According to the precondition, the geometric parameter of Bennett linkage ABCD is

$$a_{\mathrm{AB}} = a_{\mathrm{CD}} = a, \qquad a_{\mathrm{AD}} = a_{\mathrm{BC}} = b,$$

$$\alpha_{\mathrm{AB}} = \alpha_{\mathrm{CD}} = \alpha, \qquad \alpha_{\mathrm{AD}} = \alpha_{\mathrm{BC}} = \beta.$$

Its kinematic variables, θ and φ, are given in figure 18*a*. The cross-sectional view of the linkage on the cylinder is given in figure 18*b*, in which the angle between planes ABD and BCD is denoted by ξ. Take l_0 as the length BD. In ΔABD,

$$l_0 = \mathrm{BD} = \sqrt{a^2 + b^2 + 2ab\cos\theta}. \tag{4.1}$$

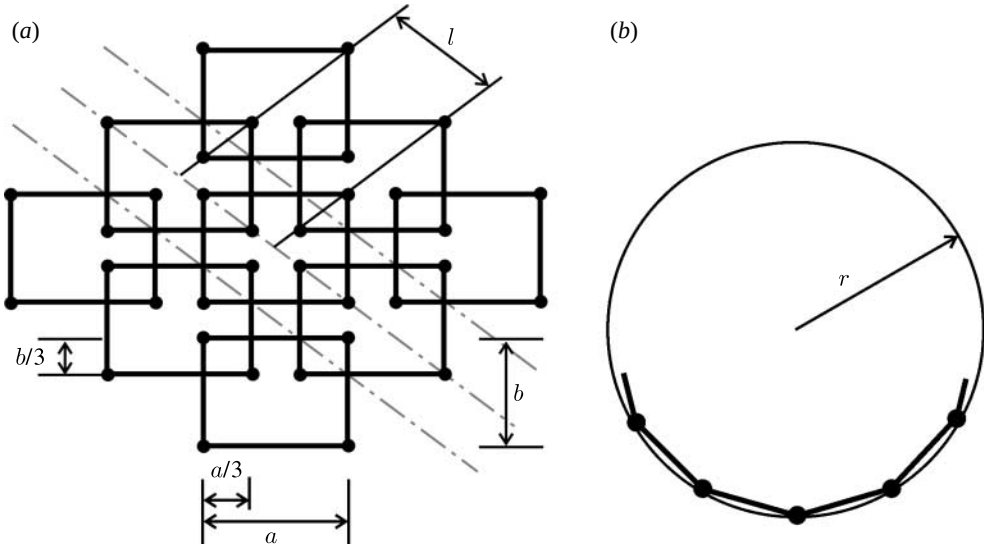

Figure 17. (*a*) Key geometrical parameters of an assembly. (*b*) The cross-sectional view.

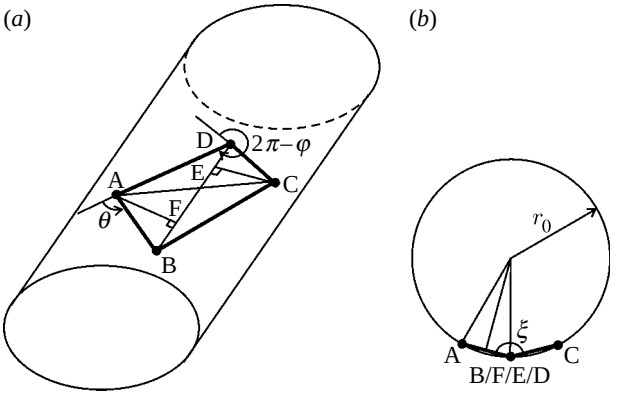

Figure 18. The geometry of a single Bennett linkage. (*a*) On the surface of a cylinder and (*b*) the cross-section view.

Denote the radius of this cylinder by r_0,

$$r_0 = \frac{1}{2}\frac{\mathrm{AF}}{\cos\frac{\xi}{2}} = \frac{1}{2}\frac{\mathrm{CE}}{\cos\frac{\xi}{2}},$$

where both AF and CE are equal and perpendicular to BD. Considering ΔABD or ΔCBD, we have

$$\mathrm{AF} = \mathrm{CE} = \frac{ab\sin\theta}{\sqrt{a^2+b^2+2ab\cos\theta}}.$$

Hence, from figure 18*b*,

$$\cos\xi = -\frac{(\cos\varphi+\cos\theta)(a^2+b^2+2ab\cos\theta)}{ab\sin^2\theta} - 1,$$

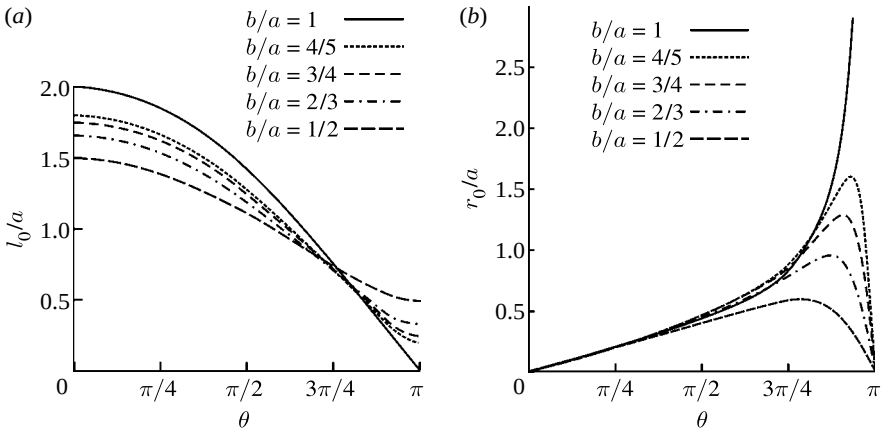

Figure 19. The geometrical parameters of a Bennett linkage when $\alpha=\pi/3$. (*a*) l_0/a versus θ and (*b*) r_0/a versus θ for various b/a.

so

$$r_0 = \frac{ab\sin^2\theta}{2(a^2+b^2+2ab\cos\theta)}\sqrt{\frac{-2ab}{\cos\theta+\cos\varphi}}. \tag{4.2}$$

Based on (4.1) and (4.2), we can plot l_0/a and r_0/a versus deployed angle θ curves. Figure 19 shows such curves for $\alpha=\pi/3$.

A few observations can be made from the diagram. Firstly, when $b/a=1$, that is, the Bennett linkage is an equilateral one, there are two folded configurations: $l_0=0$, $\theta=\pi$ and $r_0=0$, $\theta=0$. The deployment starts from a compact bundle with $r_0=0$, expands to an intermediate arch profile and finally ends when the assembly folds flat with $l_0=0$. Secondly, both the overall length and the radius of assembly change more dramatically when b/a is closer to 1. Thirdly, for assemblies made from non-equilateral Bennett linkages, when θ changes from 0 to π, l_0 decreases, whereas r_0 increases from 0 to a maximum value and then falls back to 0 again.

For each case, it is possible to establish the relationships among geometric parameters, l and r, of the assemblies, and l_0 and r_0 for the single linkage, which are listed in table 2. It is obvious that overall longitudinal length of the assembly and the radius of cylindrical profile formed by the assembly are proportional to l_0 and r_0, respectively, despite the fact that the proportion is different. The assembly of case 4 has the most compact profile, whereas the assembly of case 2 is the longest in the longitudinal direction. The assembly of case 3 offers the cylindrical profile with the largest radius, while that of cases 2 and 4 is the smallest. From our experience in making physical models, it is learnt that the assemblies with smaller radius, for example, those based on cases 2 and 4, are more likely to have conflict during the deployment, and the one with larger radius, for example, that of case 3, is much easier to be folded compactly.

5. Conclusions and discussion

In this paper, we have greatly extended our previous work on assemblies of Bennett linkages, which was published in this journal (Chen & You 2005). In total, eight cases that allow mobile assemblies of Bennett linkages to be built have been

Table 2. Geometric parameters, l and r, of the assemblies.

case	l	r
1	$(2/3)l_0$	$(2/3)r_0$
2	l_0	$(1/3)r_0$
3	$(1/3)l_0$	r_0
4	$(1/3)l_0$	$(1/3)r_0$

reported by considering the links that may contain sections with negative lengths. Among the eight assemblies, four are distinct ones, including the one that was reported previously, and the remaining can be obtained by modifying the earlier case. All of these assemblies consist of a grid of nested Bennett linkages. The layout of the assemblies can be repeated to form a large deployable structure that deploys into a cylindrical profile. When the Bennett linkages are equilateral, the assemblies form an arch profile. For non-equilateral case, the assemblies deploy into a helical shape on the cylindrical surface. They are geometrically overconstrained with a single degree of mobility.

It should be pointed out that, in all of the cases, the typical Bennett linkages in the same assembly are not necessary to be the same size, despite the fact that they look similar in size in the schematics of the paper. In fact, a mobile assembly can be obtained as long as the lengths of each Bennett linkage meet the geometric condition of the Bennett linkage (2.1*a*)–(2.1*c*), and the lengths of different linkages should also satisfy the mobile condition (2.4), which means that all the lengths of the Bennett linkages in the same assembly are proportional to each other. Also, it is possible to construct a multilayer mobile grid for cases 2–8 using the same geometrical arrangement as we did for case 1 previously (Chen & You 2005).

All of the physical models are constructed with drinking straws as links and dressmaking pins as hinges. Although, physically, they do have non-zero sectional dimensions, it seems that it is sufficient to demonstrate the mobility within the assemblies. A large model that expands to an 8 m span arch has also been constructed using carbon fibre tubes and nylon joints with embedded bearings. In this model, the locations of the joints are carefully designed so that each Bennett linkage is as perfect as the mathematical model. It expands extremely smoothly.

A number of applications for the mobile assemblies, ranging from expandable arches for rapidly deployed tents to towers, were proposed in the past. A large span rapidly deployable tent is currently under construction at the University of Oxford. The newly found configurations provide designers of such deployable structures much greater choices. The paper focuses on the geometrical features of the assemblies and therefore we have not compared the load bearing capacity of the assemblies in each case. By observation, it seems that the assembly of case 4 has the best load-carrying capacity, whereas that of case 3 could be the weakest under the radial loads. However, this has yet to be proved by detailed analysis, which is being undertaken presently.

We have also shown that the structures based on case 1 can be folded up completely to a bundle for transportation (Chen & You 2006, 2007*a*,*b*). It is believed that the same may also be applied to the other cases.

Y.C. would like to thank the Nanyang Technological University, Singapore, for providing a research grant (RG21/05) and subsequent academic leave to undertake work related to this article. Z.Y. would like to acknowledge financial support from the Engineering and Physical Sciences Research Council (grant no. EP/E502903).

References

Baker, J. E. 1979 The Bennett, Goldberg and Myard linkages—in perspective. *Mech. Mach. Theory* **14**, 239–253. (doi:10.1016/0094-114X(79)90011-9)

Baker, J. E. 1988 The Bennett linkage and its associated quadric surfaces. *Mech. Mach. Theory* **23**, 147–156. (doi:10.1016/0094-114X(88)90092-4)

Beggs, J. S. 1966 *Advanced mechanism*. New York, NY: Macmillan Company.

Bennett, G. T. 1903 A new mechanism. *Engineering* **76**, 777–778.

Bennett, G. T. 1914 The skew isogram mechanism. *Proc. Lond. Math. Soc.* **13**, 151–173. (doi:10.1112/plms/s2-13.1.151)

Chen, Y. 2003 Design of structural mechanism. DPhil (PhD) thesis, University of Oxford.

Chen, Y. & You, Z. 2005 Mobile assemblies based on the Bennett linkage. *Proc. R. Soc. A* **461**, 1229–1245. (doi:10.1098/rspa.2004.1383)

Chen, Y. & You, Z. 2006 Square deployable frame for space application: part I: theory. *Proc. Inst. Mech. Eng. Part G: J. Aerosp. Eng.* **220**, 347–354. (doi:10.1243/09544100JAERO68)

Chen, Y. & You, Z. 2007*a* Square deployable frame for space applications: part II: realisation. *Proc. Inst. Mech. Eng. Part G: J. Aerosp. Eng* **221**, 37–45. (doi:10.1243/09544100JAERO100)

Chen, Y. & You, Z. 2007*b* Deployable frames with curved profile. In *48th AIAA/ASME/ASCE/AHS/ASC Structures, Structural Dynamics and Material Conference and Exhibit, Hawaii, April 2007*, AIAA-2007-2115.

Dietmaier, P. 1995 A new 6*R* space mechanism. In *Proc. 9th World Congress IFToMM, Milano*, vol. 1, pp. 52–56.

Goldberg, M. 1943 New five-bar and six-bar linkages in three dimensions. *Trans. ASME* **65**, 649–663.

Ho, C. Y. 1978 Note on the existence of Bennett mechanism. *Mech. Mach. Theory* **13**, 269–271. (doi:10.1016/0094-114X(78)90050-2)

Huang, C. 1997 The cylindroid associated with finite motions of the Bennett mechanism. *Trans. ASME, J. Eng. Ind.* **119**, 521–524.

Mavroidis, C. & Roth, B. 1994 Analysis and synthesis of overconstrained mechanism. In *Proc. 1994 ASME Design Technical Conference, Minneapolis, MI, September*, pp. 115–133.

Myard, F. E. 1931 Contribution à la géométrie des systèmes articulés. *Societe Mathématiques de France* **59**, 183–210.

Waldron, K. J. 1968 Hybrid overconstrained linkages. *J. Mech.* **3**, 73–78. (doi:10.1016/0022-2569(68)90016-5)

Wohlhart, K. 1991 Merging two general Goldberg 5*R* linkages to obtain a new 6*R* space mechanism. *Mech. Mach. Theory* **26**, 659–668. (doi:10.1016/0094-114X(91)90028-3)

Yu, H.-C. 1981 The Bennett linkage, its associated tetrahedron and the hyperboloid of its axes. *Mech. Mach. Theory* **16**, 105–114. (doi:10.1016/0094-114X(81)90056-2)

PROCEEDINGS OF THE ROYAL SOCIETY A MATHEMATICAL, PHYSICAL & ENGINEERING SCIENCES